

AD-A017 040

**AN ANALYTICAL MODEL FOR DETERMINING ENERGY  
DISSIPATION IN DYNAMICALLY LOADED STRUCTURES**

John F. McNamara, et al

Army Construction Engineering Research Laboratory  
Champaign, Illinois

October 1975

DISTRIBUTED BY:

**NTIS**

**National Technical Information Service  
U. S. DEPARTMENT OF COMMERCE**

321128

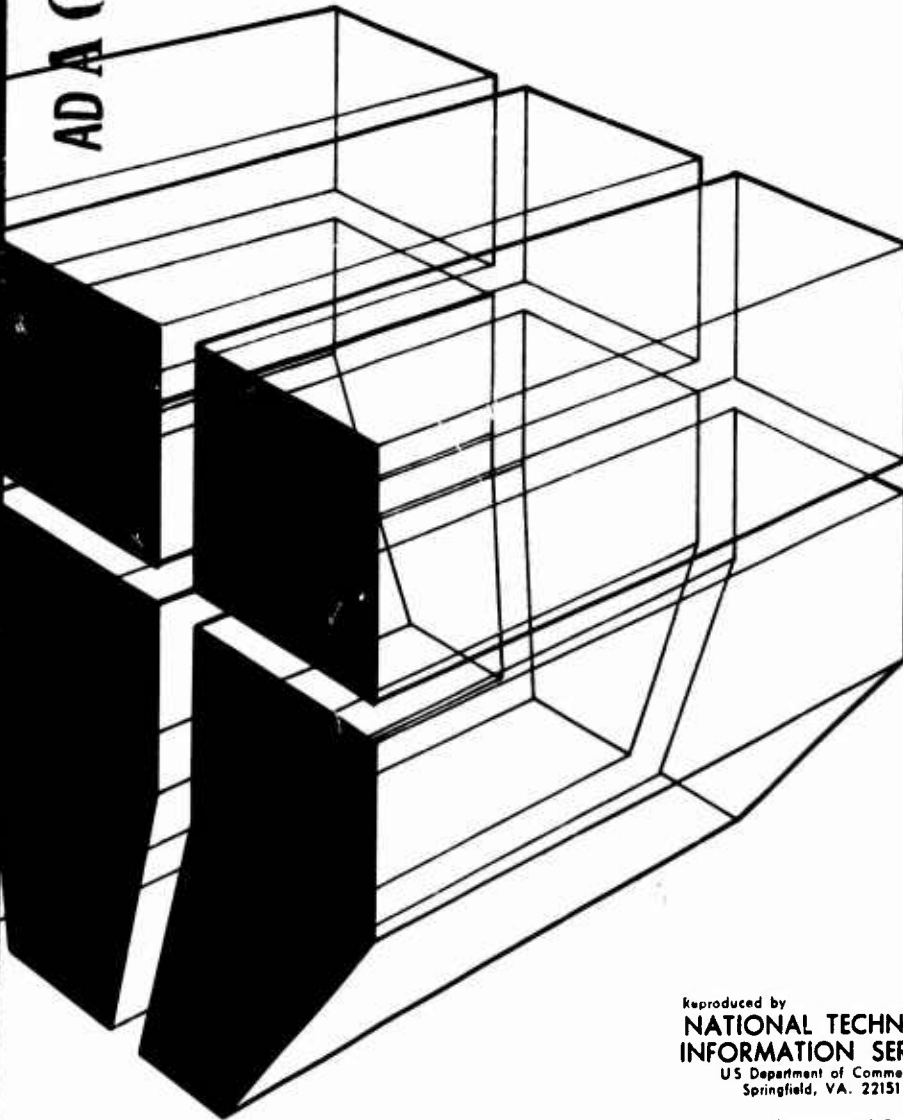
construction  
engineering  
research  
laboratory

TECHNICAL MANUSCRIPT M-165  
October 1975

ADA017040

**AN ANALYTICAL MODEL FOR DETERMINING  
ENERGY DISSIPATION IN DYNAMICALLY  
LOADED STRUCTURES**

by  
**John F. McNamara  
Sushil K. Sharma**



Reproduced by  
**NATIONAL TECHNICAL  
INFORMATION SERVICE**  
US Department of Commerce  
Springfield, VA. 22151



**Approved for public release; distribution unlimited.**

The contents of this report are not to be used for advertising, publication, or promotional purposes. Citation of trade names does not constitute an official indorsement or approval of the use of such commercial products. The findings of this report are not to be construed as an official Department of the Army position, unless so designated by other authorized documents.

ACCESSION for

NTIS  Write Section  
DTC  Built Section

QUALITIES  
JUSTIFICATION

BY  
DISTRIBUTION AVAILABILITY CODES

Dist. Avail. Code or SYMBOL

A		
---	--	--

**DESTROY THIS REPORT WHEN IT IS NO LONGER NEEDED  
DO NOT RETURN IT TO THE ORIGINATOR**

UNCLASSIFIED

SECURITY CLASSIFICATION OF THIS PAGE (When Data Entered)

REPORT DOCUMENTATION PAGE		READ INSTRUCTIONS BEFORE COMPLETING FORM
1 REPORT NUMBER CERL-TM-M-165	2 GOVT ACCESSION NO	3 RECIPIENT'S CATALOG NUMBER
4 TITLE (and Subtitle) AN ANALYTICAL MODEL FOR DETERMINING ENERGY DISSIPATION IN DYNAMICALLY LOADED STRUCTURES		5 TYPE OF REPORT & PERIOD COVERED
7 AUTHOR(s) John F. McNamara Sushil K. Sharma		6 PERFORMING ORG. REPORT NUMBER
9 PERFORMING ORGANIZATION NAME AND ADDRESS CONSTRUCTION ENGINEERING RESEARCH LABORATORY P.O. Box 4005 Champaign, Illinois 61820		8 CONTRACT OR GRANT NUMBER(s)
11 CONTROLLING OFFICE NAME AND ADDRESS		10 PROGRAM ELEMENT, PROJECT, TASK AREA & WORK UNIT NUMBERS
14 MONITORING AGENCY NAME & ADDRESS (if different from Controlling Office)		12 REPORT DATE October 1975
		13 NUMBER OF PAGES * 37
		15 SECURITY CLASS (of this report) UNCLASSIFIED
		15a DECLASSIFICATION/DOWNGRADING SCHEDULE
16 DISTRIBUTION STATEMENT (of this Report)  Approved for public release; distribution unlimited.		
17 DISTRIBUTION STATEMENT (of the abstract entered in Block 20, if different from Report)		
18 SUPPLEMENTARY NOTES		
19 KEY WORDS (Continue on reverse side if necessary and identify by block number)  energy dissipation analytical simulation model dynamic loading		
20 ABSTRACT (Continue on reverse side if necessary and identify by block number) An analytical procedure is developed which predicts nonlinear cyclic structural response under large reversals of plastic strains. The structure is discretized by means of the finite element approximation, and the material behavior is simulated by a refined analytical model which describes the realistic hysteretic stress-strain curves of A36 steel under arbitrary cycles of load. In order to test the validity of this material model some comparisons are made with experimental		

UD FORM 1473 1 JAN 73 EDITION OF 1 NOV 65 IS OBSOLETE

UNCLASSIFIED

SECURITY CLASSIFICATION OF THIS PAGE (When Data Entered)

1

**UNCLASSIFIED**

SECURITY CLASSIFICATION OF THIS PAGE (When Data Entered)

values of the inelastic response of a simply supported beam under cyclic bending. The model is subsequently used in the dynamic analysis of a portal frame subjected to a selection portion of the El Centro NS earthquake acceleration record. The improved cyclic response with the current approach is illustrated by comparing results with those obtained using a simple bilinear kinematic hardening material approximation. Comparisons are also made with values obtained using a commercially available nonlinear frame analysis computer program. Some final comments are made regarding the rate of solution convergence with integration time step size for two different temporal integration operators used in this analysis.

2

**UNCLASSIFIED**

SECURITY CLASSIFICATION OF THIS PAGE (When Data Entered)

## FOREWORD

This paper was presented at the Sixth Joint Meeting of the U.S. - Japan Panel on Wind and Seismic Effects, May 1974, Gaithersburg, Maryland.

John F. McNamara is an Assistant Professor of Civil Engineering at the University of Illinois and a research engineer (IPA) at the U.S. Army Construction Engineering Research Laboratory, Champaign, Illinois. Sushil K. Sharma is a Research Assistant in the Department of Theoretical and Applied Mechanics, University of Illinois, and is an IPA at CERL.

The authors wish to thank Dr. F. B. Plummer, ESSO Production Research Co., Houston, Texas, for his assistance in inserting his computer model of material behavior into their program.

COL M. D. Remus is Commander and Director of CERL, and Dr. L. R. Shaffer is Deputy Director. Dr. W. E. Fisher is Chief of the Structural Mechanics Branch and Acting Chief of the Materials Systems and Science Division.

## CONTENTS

	DD FORM 1473	1
	FOREWORD	3
	LIST OF TABLES	5
1	INTRODUCTION	7
2	METHOD OF ANALYSIS	9
3	NUMERICAL RESULTS	17
4	CONCLUSIONS	31
	APPENDIX	32
	REFERENCES	34
	DISTRIBUTION	

## LIST OF FIGURES

<u>Number</u>		<u>Page</u>
1	Stress-Strain Response of the Series Model	13
2	"Stable" Hysteresis Loops for A36 Steel With a Common Origin	15
3	Hysteresis Loop Branches Fitted to the Skeleton Curve	16
4	Predicted and Experimental Stress-Strain Behavior for Virgin A36 Steel	18
5	Experimental Program	19
6	Comparison of Beam Finite Element Results With Experimental Values	21
7	Comparison of Plane Stress and Beam Finite Element Results for Cyclic Material Model	22
8	Response of Portal Frame to El Centro Earthquake	27
9	Response of Portal Frame to Sinusoidal Base Motion	28
10	Newmark Operator ( $\beta = 1/4$ ) with $\Delta T = 0.005$ and $\Delta T = 0.0025$	30



## 1 INTRODUCTION

The dynamic analysis of framed steel structures under earthquake loading would appear to be well in hand, and many studies and applicable computer programs are readily available [1,2,3].\* In terms of building configuration, structural elements, and applied loading, the programs are general in nature, but all assume that material behavior can be approximated in terms of moment-rotation joint relationships. A simple bilinear or Ramberg-Osgood [2,4,5] curve fit is usually adapted to model this material resistance function and appears adequate for most engineering applications. Currently accepted design criteria for steel structures with respect to lateral displacements, ductility ratios, and lateral forces have evolved from studies using the above computer programs. However, the complexity of the load-displacement hysteresis loops for frame type structures, where buckling, plastic straining, large displacements and joint slip are active, can be judged from the survey given in [6] of computations and experiments on model structures.

The current study presents some results obtained during the course of a continuing research project on the magnitude and distribution of energy dissipation in dynamically loaded structures. A significant point of this research is that the behavior of the structure is found by means of a material model with properties derived from the exact hysteretic stress-strain behavior of A36 steel. Measurements of the cyclic behavior of A36 steel were carried out in [8], and the analytical model was developed and validated in [7] for uniaxial and multiaxial stress states. By means of this model, one can incorporate the results of advanced research in material behavior

---

\*Bracketed numbers refer to reference list.

into engineering analysis. In all cases known to the writers, cyclic material behavior has been deduced from monotonic test curves while, in fact, highly accurate results on cyclic behavior are readily available [9,10,11]. The development of this higher order material model supplements the current activity in the cyclic testing of structures through large strain reversals [12].

Since the material resistance is synthesized from knowledge of a pointwise stress-strain relation rather than a moment-rotation relation at a joint, the finite element method rather than a stiffness method is used to model the structure. The element used is a simple beam-column with the stiffness matrix obtained by numerical integration along the length and through the depth of a member element. A finite element plane stress analysis of a simply supported beam, cycled through three load reversals with large plastic strains, was used in [7] to check the material model under discussion. Further analysis of the same problem, using a beam-column element and idealized material properties, is given in [13]. The purpose of the study in [13] was an assessment of the accuracy of numerical solution techniques with a particular reference to cyclic loading. The refined material model has been incorporated in a general purpose finite element computer program [14] capable of analyzing the nonlinear static and dynamic responses of engineering structures.

The objective of this research is to formulate an analytical procedure for determining overall structural energy dissipation properties on the basis of experimental cyclic material behavior. A projected use of the numerical results is an assessment of the effect of nonlinear material behavior on the damping properties of structures.

The preliminary results given here are aimed at verifying the overall analytical model and the accuracy of the numerical solution procedures. For the case of a simple portal frame under earthquake excitation it is shown that considerable differences in displacement values occur between the current results and those obtained using a bilinear kinematic hardening stress-strain relation.

## 2 METHOD OF ANALYSIS

### (i) Finite Element Formulation

The general equation of motion for a body, derived from the principle of virtual work, is written in terms of initial geometry as

$$[M] \{\ddot{q}_t\} = - \int_V [B]^T \{S\} dV + \{P_t\} \quad (1)$$

where  $[M]$  is a consistent or diagonal mass matrix.  $\{q\}$ ,  $\{\ddot{q}\}$  are the generalized displacement and acceleration vectors.  $\{P\}$  is a vector of equivalent nodal forces.  $\{S\}$  is a vector of generalized stresses.

The matrix  $[B]$  transforms generalized displacement increments at the nodes to generalized strain increments at any point in an element. It is defined by the equation

$$\{\Delta E\} = [B] \{\Delta q\} \quad (2)$$

and is a nonlinear function of displacement. The expressions used in forming  $[B]$  in the current study are given in the Appendix.

A modified, or corrected, linear incremental form [14] of Eq. (1) is obtained as

$$\begin{aligned}
[M] \{\Delta \ddot{q}_{t+\Delta t}\} = & - \int_V [\Delta B]^T \{S\} dV - \int_V [B]^T \{\Delta S\} dV + \{\Delta P_{t+\Delta t}\} \\
& + (-[M]\{\ddot{q}_t\} - \int_V [B]^T \{S\} dV + \{P_t\})
\end{aligned} \quad (3)$$

The incremental stress vector  $\{\Delta S\}$  can be expressed in terms of  $\{\Delta q\}$  by using Eq. (2) and the following linear incremental stress-strain relation

$$\{\Delta S\} = [D_{ep}] \{\Delta E\} \quad (4)$$

The construction of the elastic-plastic stress-strain transformation matrix  $[D_{ep}]$  with reference to the new material model follows the approach outlined in [15]. By substituting Eq. (4) in Eq. (3) and following procedures described in [15], Eq. (3) can be written as

$$[M] \{\Delta \ddot{q}_{t+\Delta t}\} = - [K_t] \{\Delta q_{t+\Delta t}\} + \{\Delta P_{t+\Delta t}\} + \{I_t\} \quad (5)$$

where the tangential stiffness matrix  $[K_t]$  is formed by combining the first two integrals on the right hand side of Eq. (3), and the "load correction term"  $\{I_t\}$  is the contribution of the terms inside the parenthesis in Eq. (3).  $\{I_t\}$  is the total unbalanced force at time  $t$ .

#### (ii) Time Integration

The controversy over an optimum temporal integration operator has produced a large volume of studies in recent years. Direct methods [16] are available for estimating the accuracy of these operators when applied to linear systems [17], but it seems that only numerical experiments can provide a measure of their worth in the nonlinear case. In a recent analysis [18] of the performance of several popular operators (namely the Houbolt [19], the Wilson [20], the Newmark Beta [21], and the central difference operator), it was noted that the

accuracy and stability of solutions with these operators were very different between corresponding linear and nonlinear applications. The overall conclusion arrived at in [18] is that inaccuracies in nonlinear solutions accumulate very rapidly when integration operators are used with time increments larger than that of the stability limit given by the central difference operator.

In order to further investigate the result described above, both the central difference operator and the Newmark operator with  $\beta=1/4$  and  $\gamma=1/2$  were used in the current study. The latter operator is generally applied in earthquake engineering and is the basis of the solution method in [3]. The incremental value of the displacement vector is given by the central difference operator as

$$\{\Delta q_t\} = \{\Delta q_{t-\Delta t}\} + \Delta t^2 \{\ddot{q}_{t-\Delta t}\} \quad (6)$$

The solution cycle is formed by calculating the displacement increment from Eq. (6) and using this value to compute the integral on the right hand side of Eq. (1). The acceleration for the next step is found by solving Eq. (1) for  $\{\ddot{q}_t\}$ . The operator is not self-starting and suitable initial values are outlined in [18].

Because of its implicit form, the Newmark operator is more conveniently combined with a linearized equation of motion such as given by Eq. (5). The increment of acceleration is given by

$$\{\Delta \ddot{q}_{t+\Delta t}\} = \frac{1}{4\Delta t^2} (\{\Delta q_{t+\Delta t}\} - \Delta t \{\dot{q}_t\} - \frac{\Delta t^2}{2} \{\ddot{q}_t\}) \quad (7)$$

Substitution of Eq. (7) into Eq. (5) yields

$$\left(\frac{4[M]}{\Delta t^2} + [K_t]\right) \{\Delta q_{t+\Delta t}\} = \{\Delta P_{t+\Delta t}\} + \{I_t\} + \frac{4[M]}{\Delta t^2} (\Delta t \{\dot{q}_t\} + \frac{\Delta t^2}{2} \{\ddot{q}_t\}) \quad (8)$$

In this approach  $\{\Delta q_{t+\Delta t}\}$  is first calculated from Eq. (8) and then substituted back into Eq. (7) to find the acceleration increment. The velocity vector is given by

$$\{\dot{q}_{t+\Delta t}\} = \{\dot{q}_t\} + \frac{\Delta t}{2} (\{\ddot{q}_t\} + \{\ddot{q}_{t+\Delta t}\}) \quad (9)$$

Damping forces of the equivalent viscous type are not included at present since they would complicate the interpretation of the effect of material nonlinearity in the response.

#### (iii) Constitutive Relation and Refined Material Model

The new refined material model is an extension of the work of Martin [22] and Jhansale [23] and is described in detail in [7,8]. A mechanical analog of the basic series model with only three elements is shown in Fig. 1. Each spring of the system has a linear stress-strain relationship. The springs in the parallel spring-slider elements are not deformed until the applied stress reaches the yield stress of the slider in that element. If the applied stress in an element reaches above the yield stress, then the difference is stored in the element as a residual stress. The tangent modulus  $E_i^*$  on a given segment of the curve is obtained from the relation

$$\frac{1}{E_i^*} = \frac{1}{E} + \sum \frac{1}{E_i} \quad (10)$$

where the summation is extended over all those spring-slider elements which have yielded. The stress-strain response with this model follows

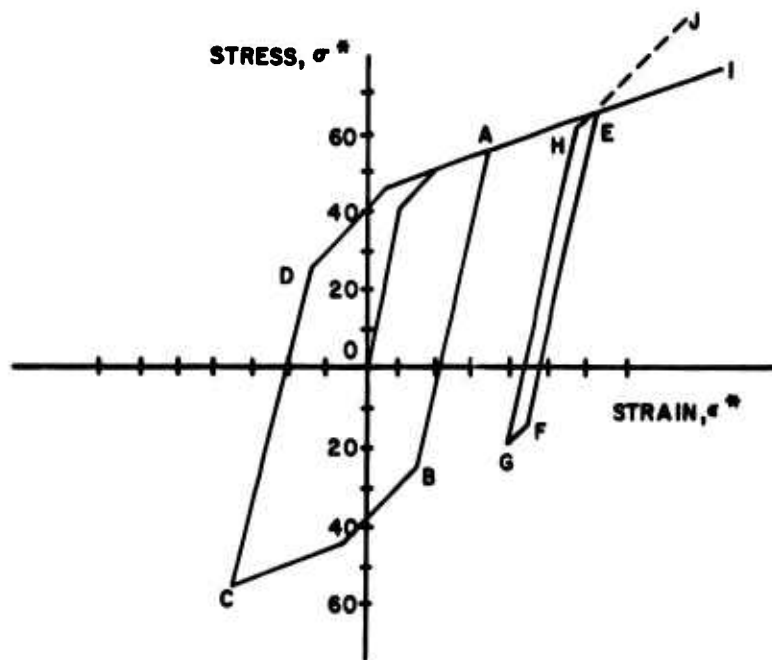


Figure 1. Stress-strain response of the series model.

Massing's hypothesis where the closed hysteresis loops are the same form as the stabilized initial branch OA of the stress-strain curve except for an enlargement by a factor of two [10]. The hypothesis also implies that after a small hysteresis loop EFGH, the loading branch will follow the path EI instead of EJ. This is an example of the "memory" effect which is created by the distribution of residual stress in the elastic springs.

This basic model cannot, however, accurately trace the hysteretic stress-strain curve of A36 steel for two reasons. Firstly, A36 steel in its "stable" condition does not obey Massing's hypothesis. This is shown in Fig. 2 where the cyclic stress-strain curve, increased by a factor of two, does not accurately describe the hysteresis loop shapes, and the upper hysteresis loop tips do not fall along the upper trace of the largest loop. Secondly, A36 steel cyclically hardens or softens before becoming stable. It was observed in [23] and [7] that even during the hardening and softening process each upper branch of stress-strain curve (except for the initial flat top branch) could be fitted to the double skeleton curve for the "stable" material by translating the loop along the elastic line. The loop is translated along the elastic line until the upper loop tip is approximately tangent to the double skeleton curve. An outer trace of a given loop is then described in terms of this skeleton curve and an appropriate stress offset,  $S_{OS}$ , which defines the amount that the loop must be displaced along the elastic line. In Fig. 3 the individual branches of hysteresis loops obtained from constant amplitude strain controlled tests have been fitted to the double skeleton curve. As shown in the figure, the stress offset,  $S_{OS}$ , depends on the number of reversals and the



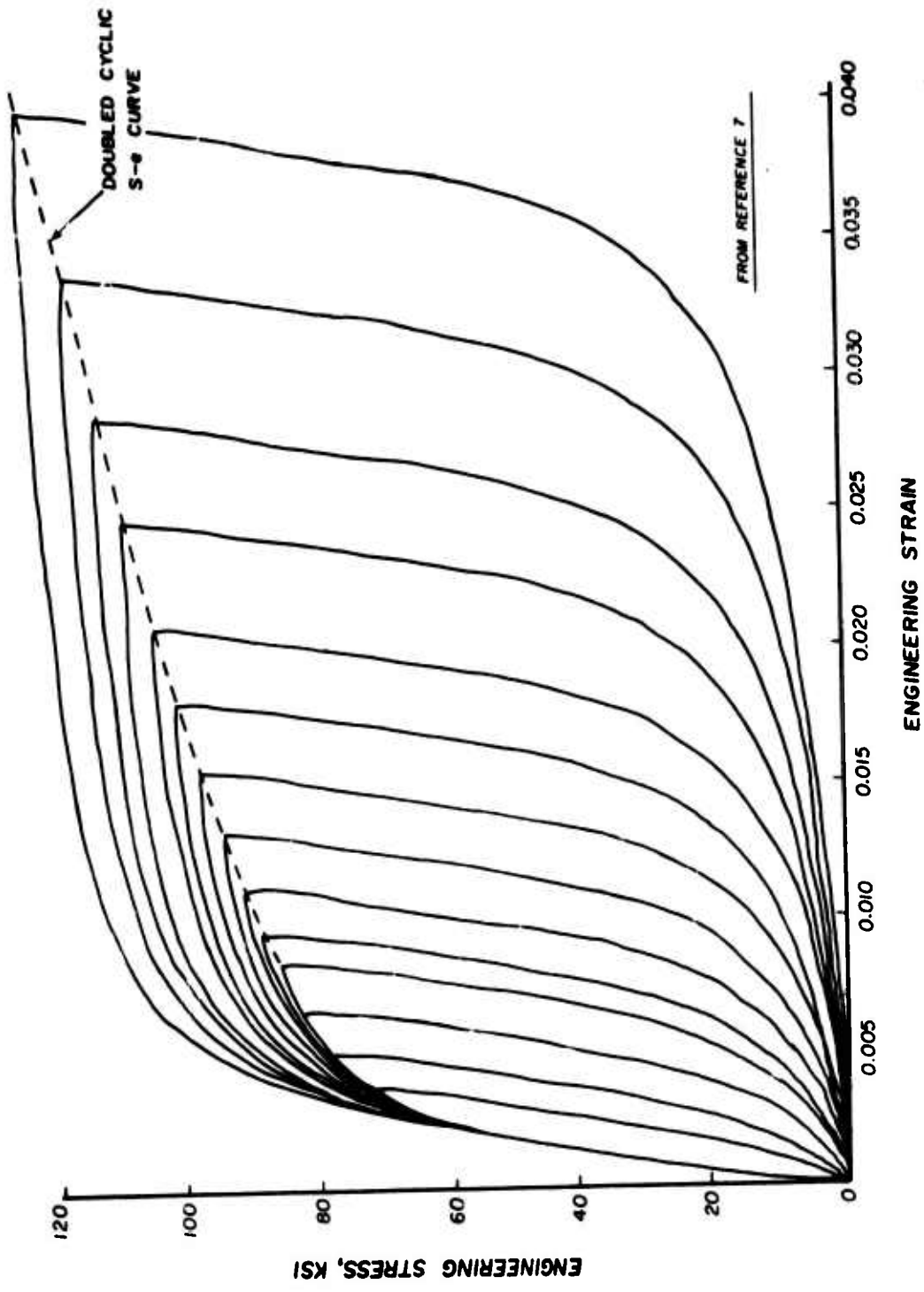


Figure 2. "Stable" hysteresis loops for A36 steel with a common origin.

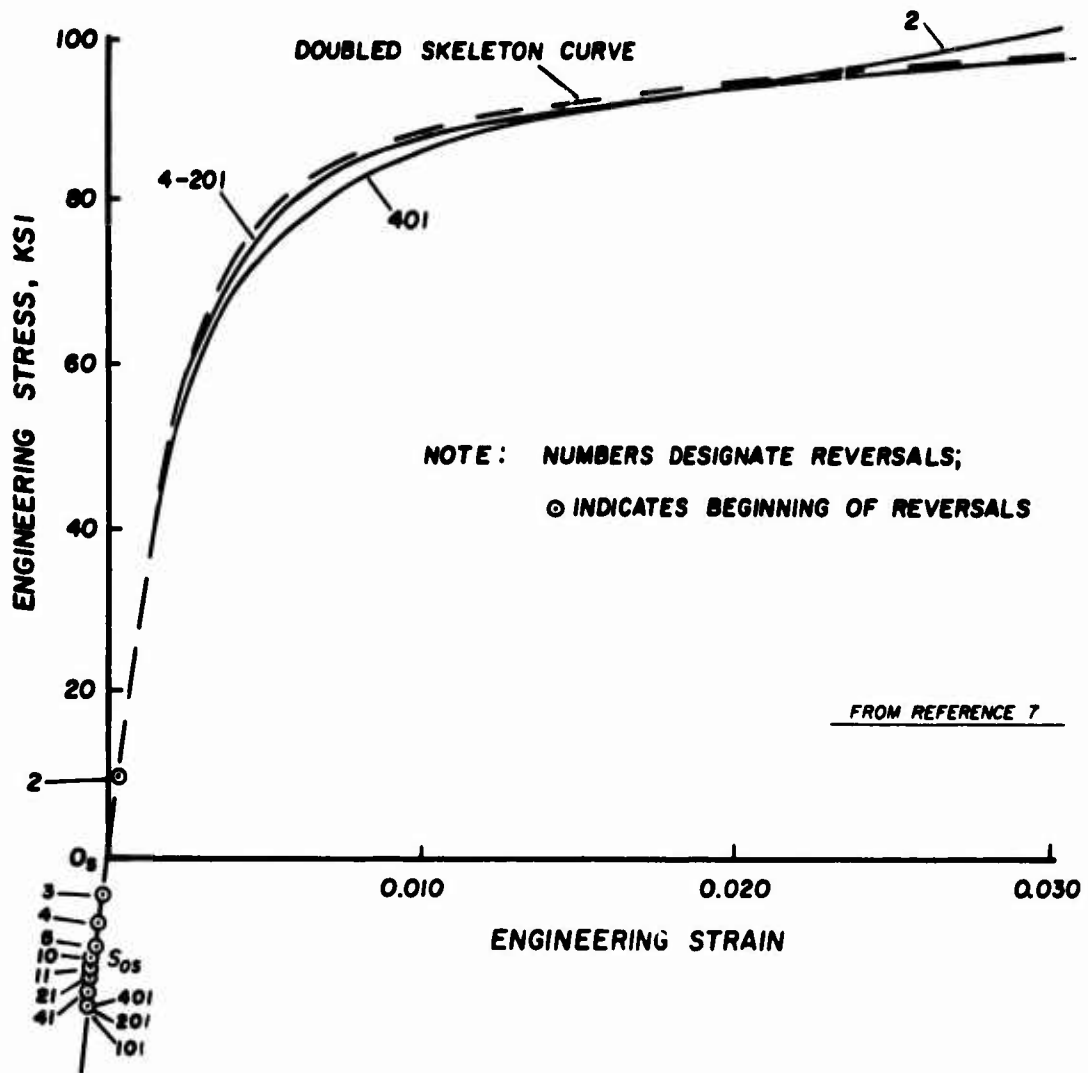


Figure 3. Hysteresis loop branches fitted to the skeleton curve.

total strain range. In this study  $S_{OS}$  is approximated by a family of linear functions of the number of reversals and the total strain range.

The analytical material model also incorporates cycle-dependent mean stress as described in [7], but this feature is not activated in the present study. An added feature is that the initial response of the model is determined by a set of constants derived from the "flat-top" stress-strain curve obtained by testing a virgin specimen of A36 steel. The spring constants and slider stress values for subsequent reversals after the first loading are found separately from the skeleton curve obtained from constant amplitude strain controlled cyclic tests of steel specimens. The procedure, used to compute the spring constants and slider stress values, is described in detail in Appendix A of [7]. Agreement between the refined material model and a complicated cyclic stress-strain history for a virgin steel is shown to be highly satisfactory by the results depicted in Fig. 4.

### 3 NUMERICAL RESULTS

#### (i) Verification of Material Model in Structural Application

In order to test the validity of the material model in structural applications the beam problem, described in Fig. 5, was developed. Ten spring-slider elements were used in the material simulation, and the dimensions of the beam were chosen in order to obtain large plastic strains without introducing nonlinear geometric effects. The beam was loaded and reloaded through three cycles as shown in Fig. 5. In the earlier investigation of Plummer [7] the beam half-span was modeled by 15 plane stress 8-node isoparametric finite elements [24]. With a view to later, more general frame-type structural applications,

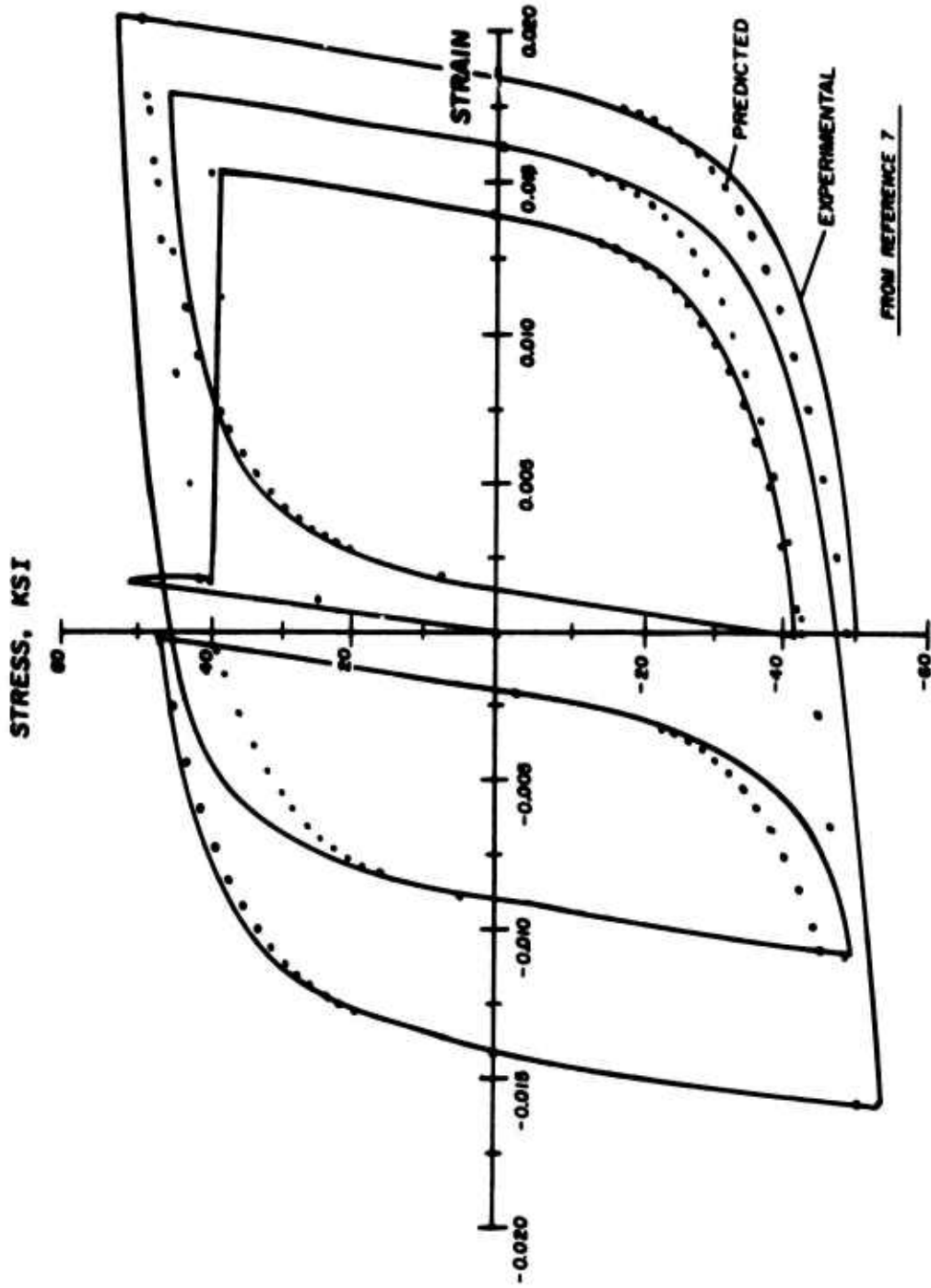
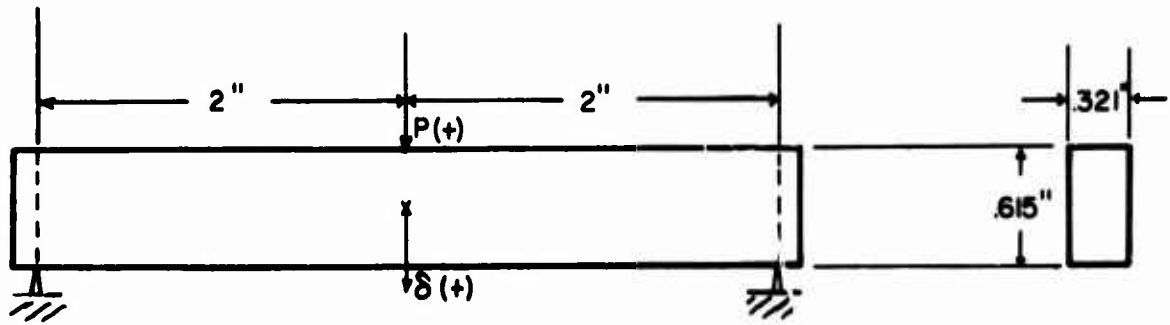


Figure 4. Predicted and experimental stress-strain behavior for virgin A36 steel.



### BEAM EXAMPLE

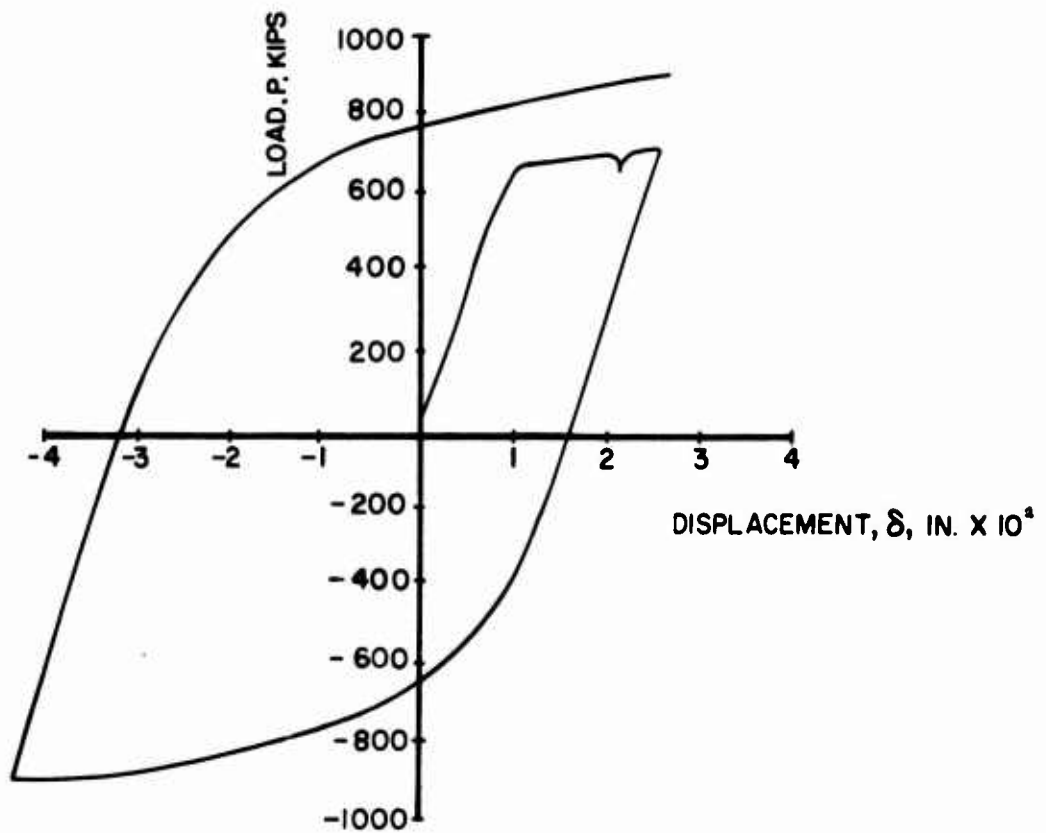


Figure 5. Experimental program.

the half-span was modeled with 10 simple beam-column elements in the present study. The generalized strain-displacement relations on which the beam-column element is based are outlined in the Appendix.

The numerical and experimental results for the beam are compared in Fig. 6. The geometric shapes of both curves are so clearly similar that it appears that a slight extension of the elastic range would allow perfect agreement. The dimensions of the beam span, cross-section, and concentrated loading also make it likely that shear deformations contribute in part to the difference in results. This is investigated in Fig. 7 where the results of the plane stress analysis from [7] are compared with the current beam-column results. The continual redistribution of the two-dimensional stress state in the plane stress results means that, even for zero hardening, the load will continue to increase after the critical mid-section has become totally plastic. In a similar example Felippa [25] found a 35 percent increase in load capacity beyond the limit load in simple bending at a displacement of approximately five times the elastic limit value. The effect in this case is to give the plane stress curve a greater slope on the initial branch which leads to higher residual stresses in the spring elements before the first reversal. The residual stresses for the beam-column case are practically zero except for one element, and this means a flatter response will occur on the subsequent reversal. It is felt that this effect rather than shear displacement causes most of the difference in results in Fig. 7 at the end of the second reversal.

These preliminary results indicate that further tuning of the analytical material model may be in order. Current suggestions in

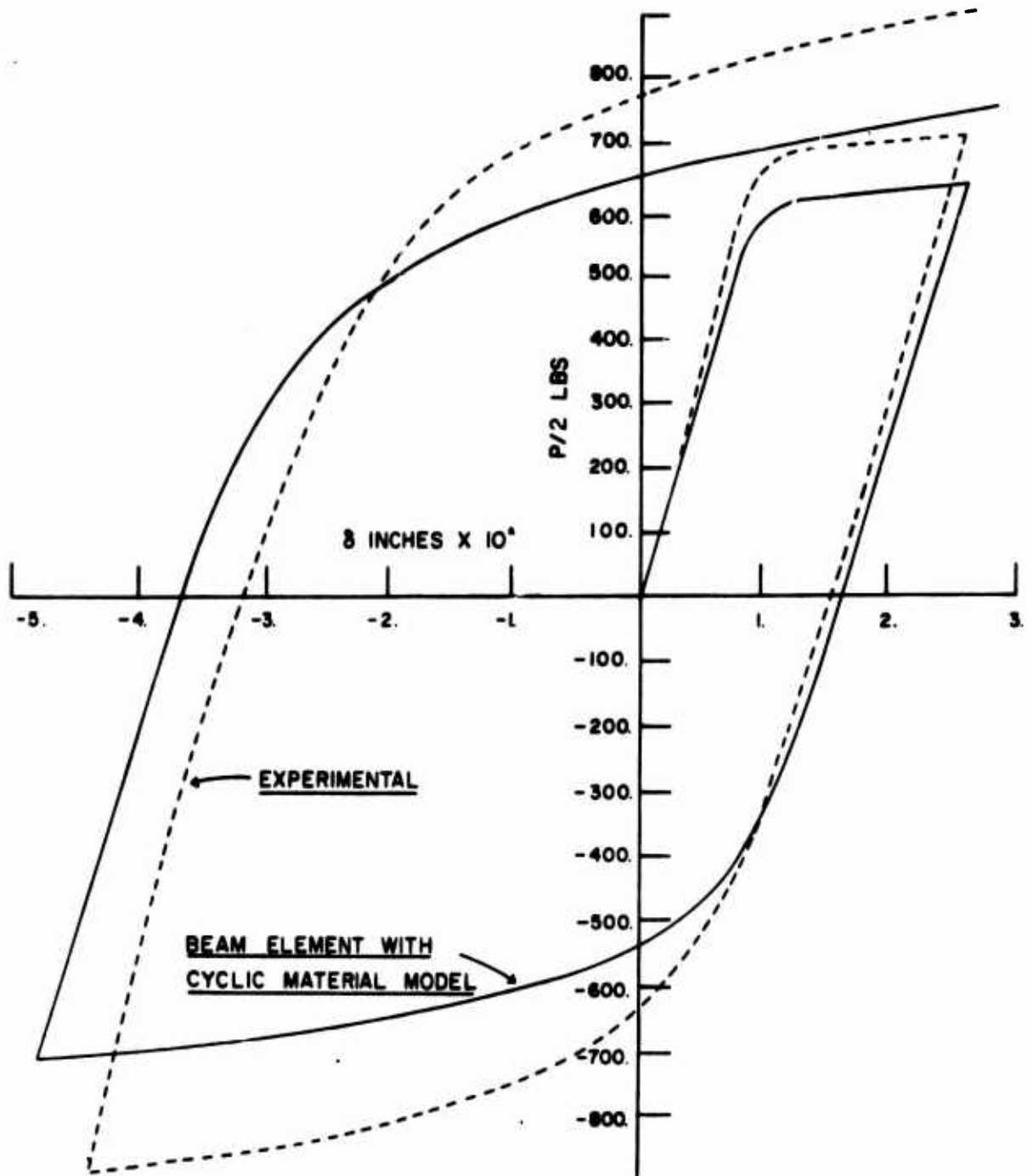


Figure 6. Comparison of beam finite element results with experimental values.

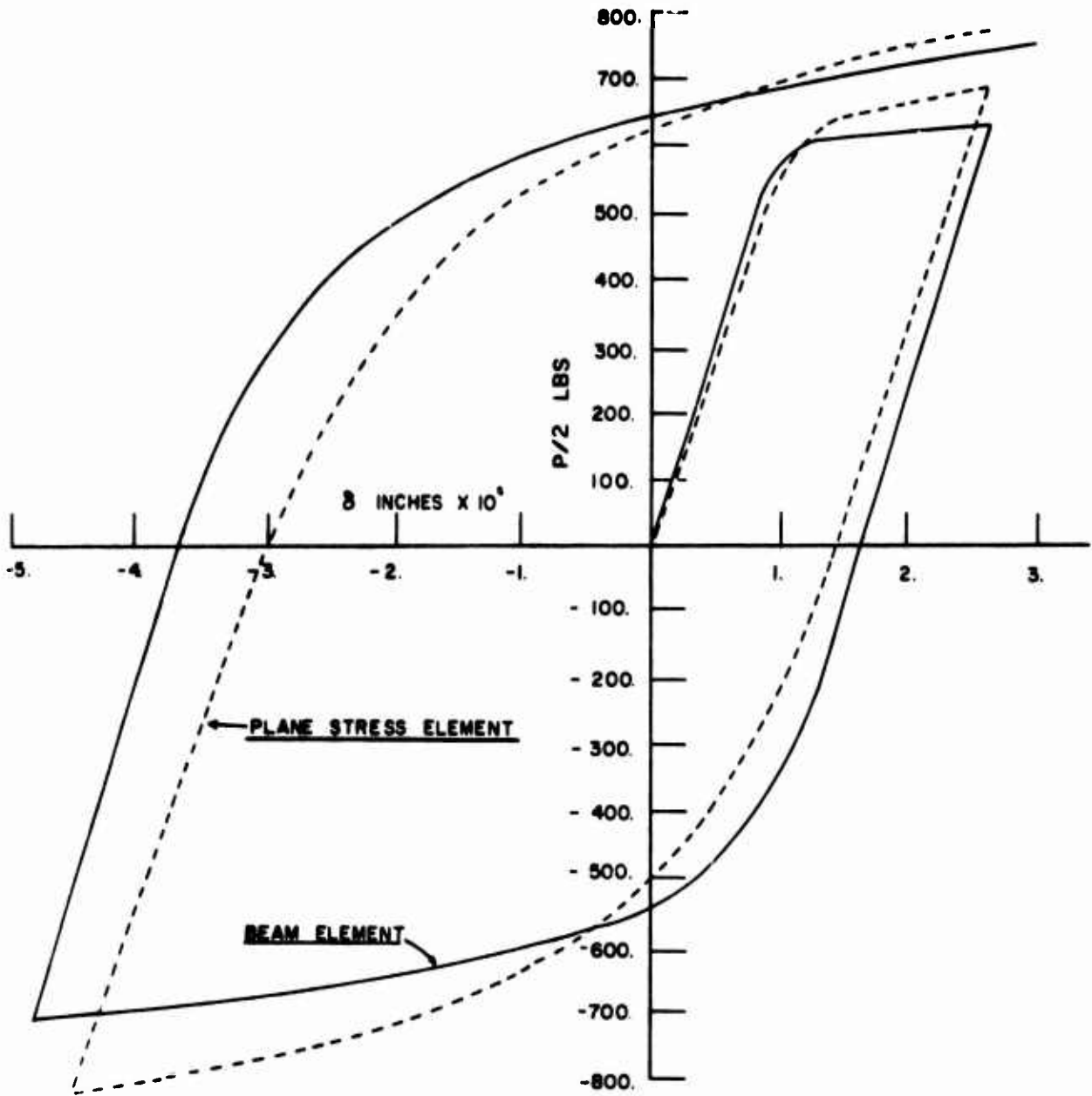


Figure 7. Comparison of plane stress and beam finite element results for cyclic material model.



this respect are to drop the initial monotonic "flat-top" behavior and use the cyclic skeleton curve for calculating one set of spring and slider values for all cases. Omission of the "flat-top" first cycle may result in an overall improved response. It was suggested in Appendix A of [7] that fictitious residual stresses be built in at the end of the "flat-top" cycle, but this may overly complicate the parameters of the model.

The constitutive relations for the plane stress analysis in [7] are based on Prager's kinematic hardening theory. This theory assumes that during plastic deformation the loading surface translates as a rigid body in stress space maintaining the size, shape and orientation of the original yield surface. Plummer [7] satisfied this constraint by not adding the stress-offset to the yield stress of the first slider. This, however, distorted the shape of the double skeleton curve represented by the spring-slider model. In the present study the stress-offset was added to the yield stress of the first slider also. A general combined kinematic-isotropic hardening theory is under active development by the writers with a view to relaxing the restriction of constant size of the loading surface.

(ii) Response of a Portal Frame to Seismic Loading

The portal frame described in [26], was modeled with three finite elements per member and subjected to a selected four seconds (1.5 sec.-5.5 sec.) of the El Centro NS earthquake acceleration record magnified by a factor of 1.5. The equations of motion must be adjusted to reflect this type of loading and Eq. (8) is replaced by

$$\begin{aligned} \left( \frac{4[M]}{\Delta t^2} + [K_t] \right) \{\Delta u_{t+\Delta t}\} &= \{\Delta P_{t+\Delta t}\} + \{I_t\} \\ &+ \frac{4[M]}{\Delta t^2} (\Delta t \{\dot{u}_t\} + \frac{\Delta t^2}{2} \{\ddot{u}_t\} - \frac{\Delta t^2}{4} \{\ddot{Q}_t\}) \end{aligned} \quad (11)$$

where  $\{\Delta u_{t+\Delta t}\}$  is now the generalized displacement relative to base of

the structure. The vector  $\{\ddot{Q}_t\}$  is formed by the components of base acceleration input. The equilibrium correction term is also changed to

$$\{I_t\} = - [M](\{\ddot{u}_t\} + \{\ddot{Q}_t\}) - \int_V [B]^T \{S\} dV + \{P_t\} \quad (12)$$

For the solution with the central difference operator, Eq. (1) is solved as it is written for the absolute acceleration, and the relative structural acceleration is obtained from the relation

$$\{\ddot{u}_t\} = \{\ddot{q}_t\} - \{\ddot{Q}_t\} \quad (13)$$

Displacements relative to the base, for the purposes of calculating internal forces, are found in the usual manner as

$$\{\Delta u_t\} = \{\Delta u_{t-\Delta t}\} + \Delta t^2 \{u_{t-\Delta t}\} \quad (14)$$

The stiffness matrix  $[K_t]$  is generated numerically using three Gaussian points along the length, and the cross-sections of the I-beams are modeled by three specially weighted integration points, one placed in each flange and one at the center. The number of points in all cases can be varied, and an option also exists which allows stresses to be computed at one or all Gaussian integration points. A diagonal mass matrix is formed in the program by collapsing all rows of the consistently formed matrix on to the diagonal. The diagonal mass matrix is used with Eq. (1) and the central difference operator, and the consistent mass matrix is used in Eq. (11) since there is no apparent computational advantage in using the diagonal form.

The dotted line in Fig. 8 indicates the response of the frame with the new material model and the central difference operator. In the same figure, the solid line passing through the triangles represents

the response with kinematic hardening idealized by a simple bilinear stress-strain curve given by  $E=30 \times 10^6$  psi,  $\sigma_y=36 \times 10^3$  psi, and  $\frac{E_T}{E} = 0.1$ . A comparison of these two curves indicate the influence of the added cyclic hardening effect in the refined material model over the idealized behavior. The results clearly demonstrate a cumulative effect as the divergence between the results increases with each reversal of the response. It is emphasized that the model structure is a simple portal frame loaded with only a fraction of a typical earthquake input, and greater differences can be expected in the analysis of more complex framed structures under an extended earthquake input.

The solid line passing through the circles in Fig. 8 shows the values given by DRAIN-2D which is a standard stiffness-type program developed by Kanaan and Powell [3]. The material response is based on a bilinear moment-rotation joint, or node, relationship, and the moment-axial force interaction diagram with shape code 2 [3] was adopted. Each frame member was divided into three equal elements, and the elastic constants and hardening modulus mentioned above were employed in the analysis. Inspection of Fig. 8 shows that the results with DRAIN-2D agree in general with those found using bilinear kinematic hardening. The divergence of these curves at the final peak values in the response may be attributed to the different yield criteria and to the manner in which the structural stiffnesses are computed in the respective computer programs. The agreement between DRAIN-2D and the results of the refined material model at the final peak displacement appears to be fortuitous since the displacement histories are considerably different up to this point.

(iii) Selection of Time Increment for the Temporal Integration Operators

For linear problems the choice of an implicit versus explicit integration operator, such as the Newmark over the central difference operator, is often governed by the fact that the latter is only conditionally stable with respect to time increment size. Also, accurate solutions with comparatively large time increments can be obtained from Newmark's operator with  $\beta=1/4$  since the amplitude of each mode is conserved [21]. However, the results obtained in [18] for a geometrically nonlinear simple beam problem showed that all implicit methods suffered serious inaccuracies for time increments greater than that found to give stable results with the central difference operator, and that the Newmark method was the worst in this respect.

In the current study the portal frame, described in Fig. 8, was subjected to a sinusoidal base excitation in order to find suitable integration time-steps for the central difference and the Newmark operator. The response was obtained with the refined material model as well as with DRAIN-2D which also uses the Newmark operator, and the results are shown in Fig. 9. The limiting stable time increment size for the central difference operator was found to be 0.0025 seconds, and an apparently stable response was obtained with the Newmark operator for a time step of 0.00625. Fig. 9 indicates clearly the problem of identifying between stable but not necessarily accurate solutions. In this case all results were in agreement up until a time of 0.45 seconds when both DRAIN-2D and the finite element solution with Newmark's method begin to diverge from the central difference solution. Therefore, it was decided to assess this phenomenon more accurately by

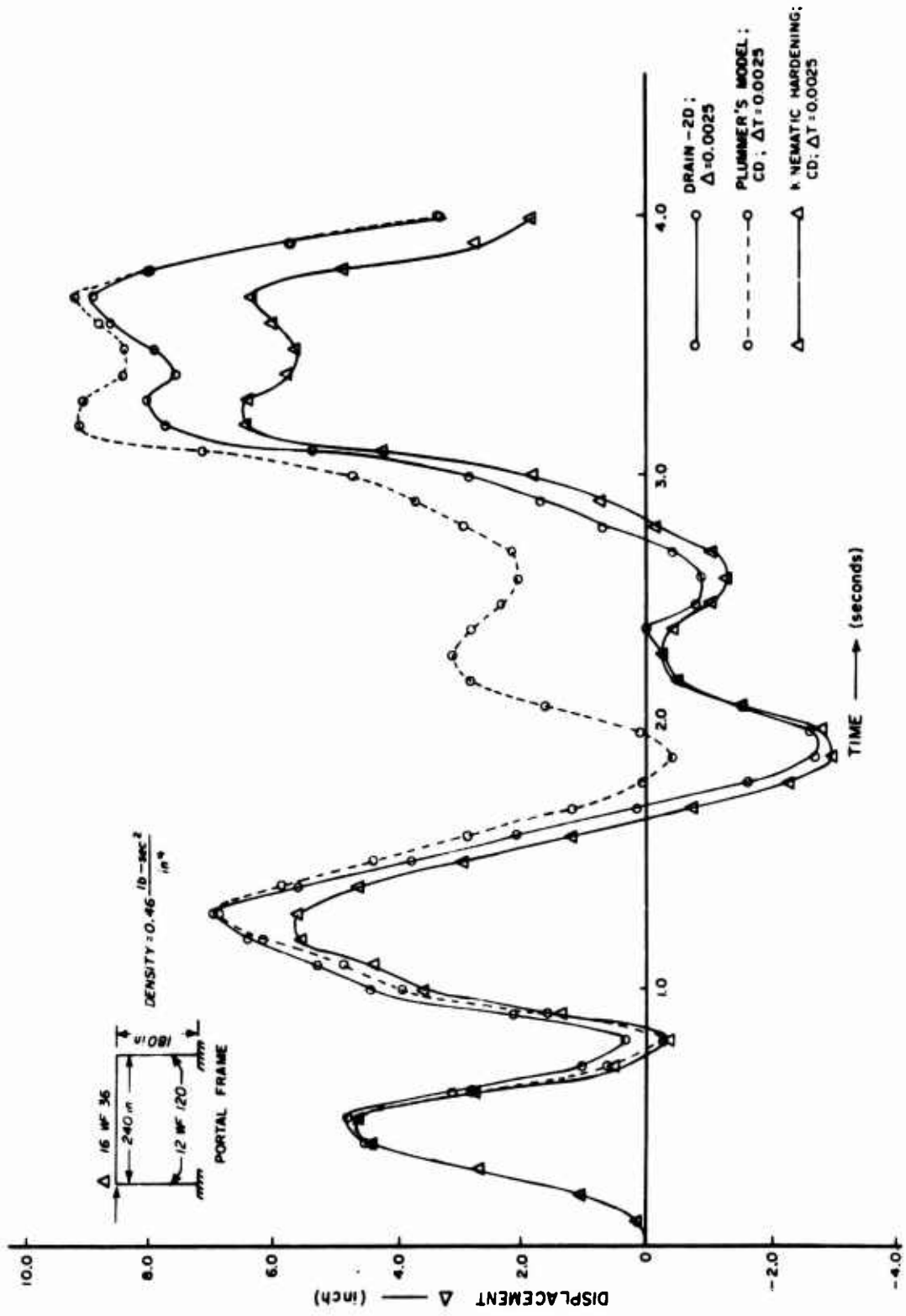


Figure 8. Response of portal frame to El Centro earthquake.

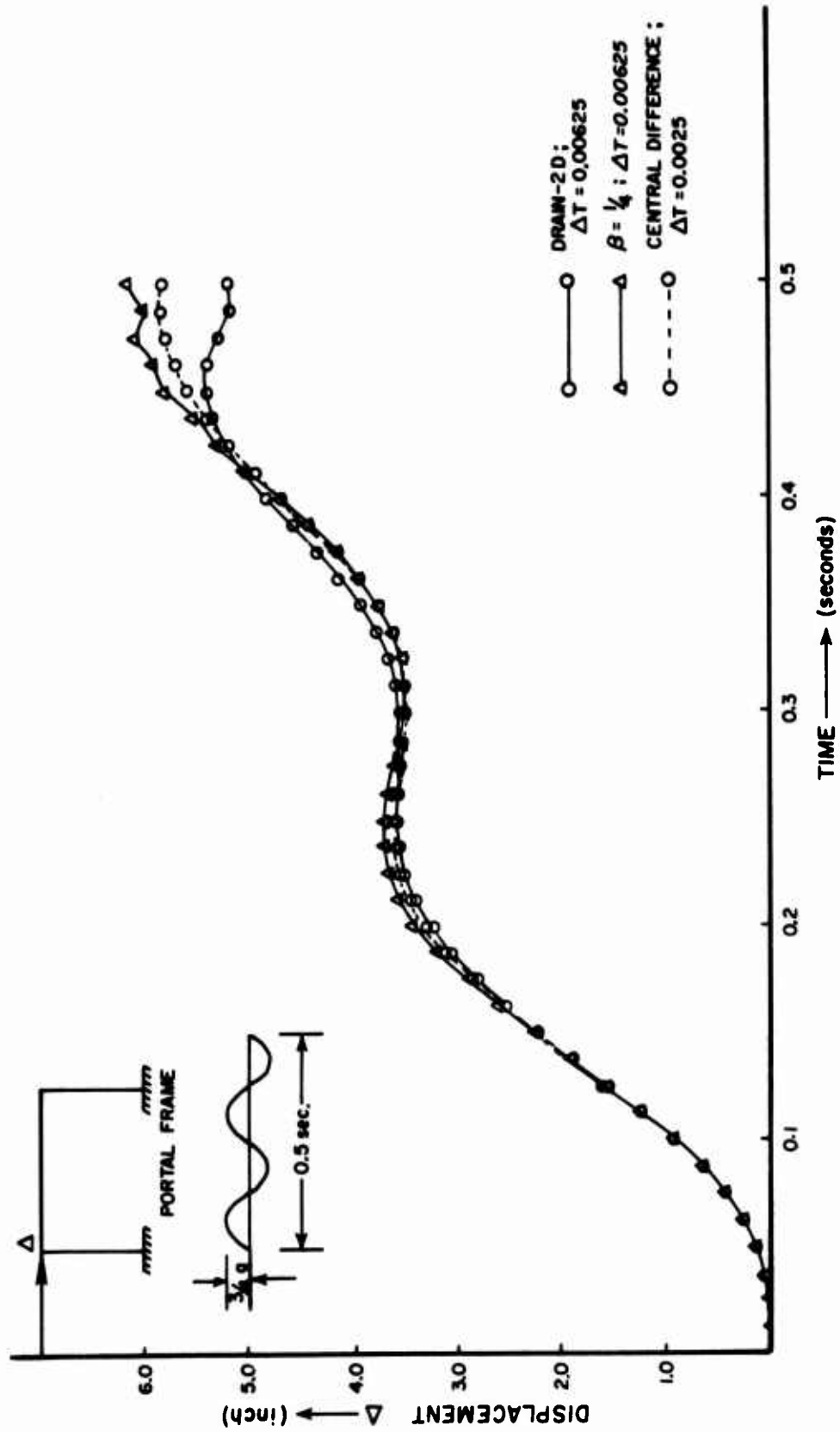


Figure 9. Response of portal frame to sinusoidal base motion.

running the problem described in Fig. 8 with decreasing time increments until convergence was achieved for the response over the time of the earthquake input. The results obtained with DRAIN-2D for increments of 0.005 and 0.0025 are shown in Fig. 10. No change occurred with a reduction in step size to .00125 and so convergence is assumed for  $\Delta t$  equal to .0025. The problem is now evident in that apparent convergence occurs over the first cycle or so with subsequent slow, but finally appreciable, divergence after approximately two seconds of the response. The recommendation is made to use the stable central difference time increment in that the seemingly apparent stability and delayed appearance of gross inaccuracies with implicit operators could lead one to believe that one had a convergent solution at larger time steps.

The results under discussion in this section, with the exception of the central difference case, were all obtained using the incremental form of the equations of motion with an elementary equilibrium, or load, correction term. It can be argued that an iterative solution at each step would improve the accuracy of the implicit solution schemes. This was attempted in [18], and for the problem studied, the iterated scheme made a difference only at those time increments which had already caused large errors, and no overall significant improvement was apparent. Further study in this respect is necessary, but the economic aspect of an explicit central difference versus an iterated implicit solution may be the deciding factor in favor of the former method. An added consideration is the simplicity of central difference solution scheme and its considerable advantage with respect to computer storage demand over the other methods.

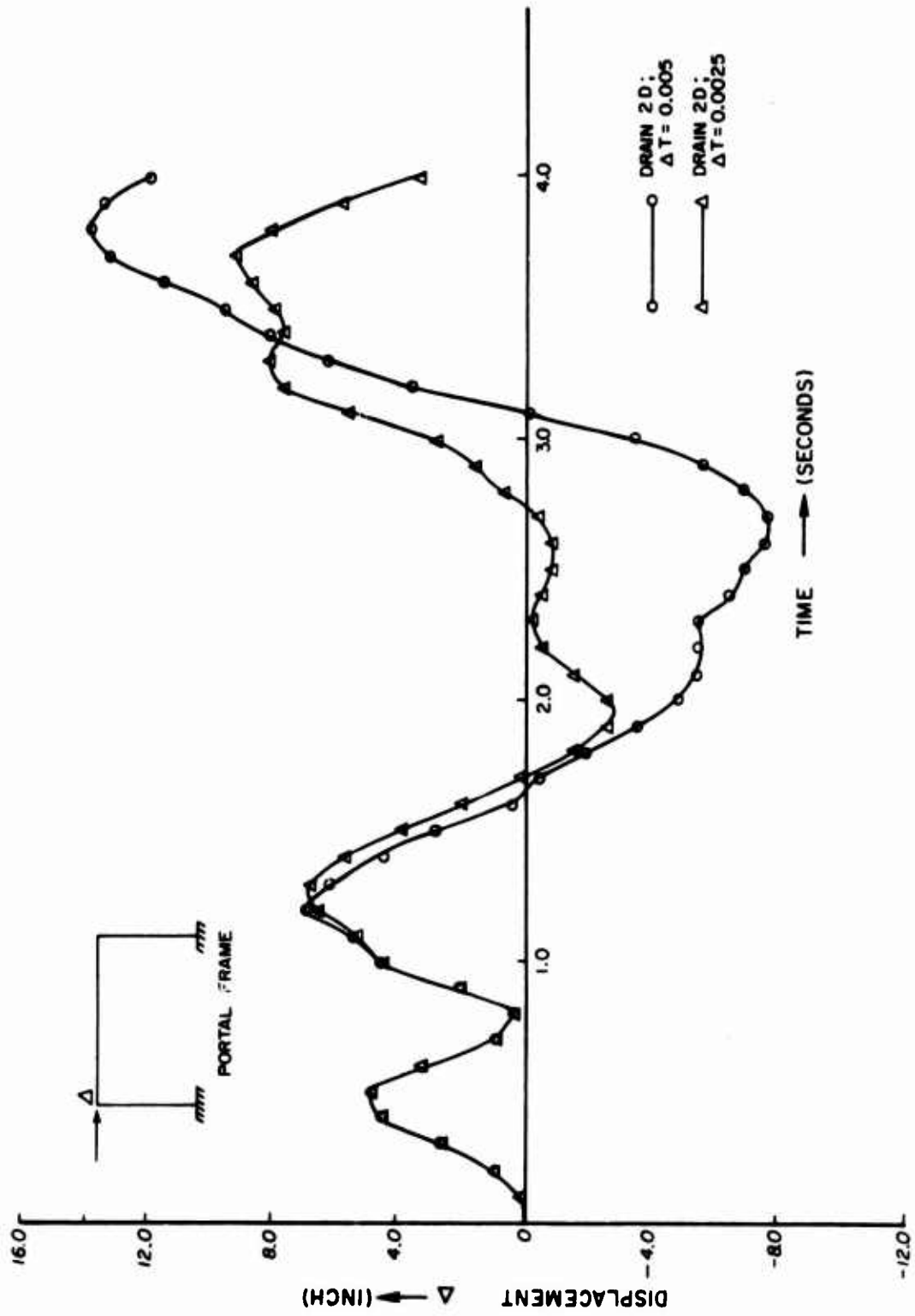


Figure 10. Newmark operator ( $\beta = 1/4$ ) with  $\Delta T = 0.005$  and  $\Delta T = 0.0025$ .



#### 4 CONCLUSIONS

An analytical procedure has been described which incorporates constitutive relations based on a higher order material model. A comparison of analytical and experimental results for a virgin A36 steel coupon and for a simply supported beam has shown the capability of the refined model to accurately predict the cyclic hysteretic material behavior.

The responses of a portal frame subjected to the El Centro NS earthquake acceleration record have been compared for the refined material model, a bilinear kinematic hardening model, and the DRAIN-2D model. The significant differences in the computed results have clearly demonstrated the effect of cyclic hardening on seismic structural response, and warrant a further study of this phenomenon with respect to energy dissipation and fatigue life of steel structures. The preliminary dynamic results suggest that for comparable accuracy the time increments for implicit integration operators and for the central difference operator must be of the same order in the case of nonlinear problems with complex time-motion histories.

## APPENDIX

BEAM-COLUMN FINITE ELEMENT

The axial and normal displacements  $U$  and  $V$  at a point  $(X, Y)$  of the beam are approximated by a linear and a cubic interpolation function of  $X$  respectively.

$$U = a_0 + a_1 X \quad (A-1)$$

$$V = b_0 + b_1 X + b_2 X^2 + b_3 X^3 \quad (A-2)$$

where  $a_0, a_1, b_0, \dots, b_3$  are generalized displacement coefficients.

It is convenient to separate the strain  $E$  at  $(X, Y)$  into its membrane and bending components  $E_m$  and  $E_b$ , where

$$E_m = \frac{dU}{dX} + \frac{1}{2} \left( \frac{dU}{dX} \right)^2 + \frac{1}{2} \left( \frac{dV}{dX} \right)^2 \quad (A-3)$$

$$E_b = -Y \frac{d^2 V}{dX^2}$$

From Eqs. (A-1) and (A-2)

$$\frac{dU}{dX} = a_1 \quad (A-4)$$

$$\frac{dV}{dX} = b_1 + 2b_2 X + 3b_3 X^2$$

An increment of strain is obtained from Eq. (A-3) as

$$\Delta E_m = \Delta \frac{dU}{dX} + \frac{dU}{dX} \left( \Delta \frac{dU}{dX} \right) + \frac{dV}{dX} \left( \Delta \frac{dV}{dX} \right) \quad (A-5)$$

$$\Delta E_b = -Y \left( \Delta \frac{d^2 V}{dX^2} \right)$$

Substituting Eq. (A-4) into (A-5),  $\Delta E_m$  and  $\Delta E_b$  can be expressed in terms of increments of generalized displacements as

$$\begin{Bmatrix} \Delta E_m \\ \Delta E_b \end{Bmatrix} = \begin{bmatrix} 0 & 1 + \frac{dU}{dX} & 0 & \frac{dV}{dX} & 2X \frac{dV}{dX} & 3X^2 \frac{dV}{dX} \\ 0 & 0 & 0 & 0 & -2Y & -6XY \end{bmatrix} \begin{Bmatrix} \Delta a_0 \\ \Delta a_1 \\ \Delta b_0 \\ \Delta b_1 \\ \Delta b_2 \\ \Delta b_3 \end{Bmatrix} \quad (\text{A-6})$$

From Eq. (A-6), matrix [B] which relates generalized incremental strains with generalized incremental displacements is readily identified as

$$[B] = \begin{bmatrix} 0 & 1 + \frac{dU}{dX} & 0 & \frac{dV}{dX} & 2X \frac{dV}{dX} & 3X^2 \frac{dV}{dX} \\ 0 & 0 & 0 & 0 & -2Y & -6XY \end{bmatrix} \quad (\text{A-7})$$

REFERENCES

1. Rea, D., Bouwkamp, J. G., and Clough, R. W., "The Dynamic Behavior of Steel Frame and Truss Buildings," American Iron and Steel Institute, Bull. No. 9, April 1968.
2. Goel, S. C., "Response of Multistory Steel Frames to Earthquake Forces," American Iron and Steel Institute, Bull. No. 12, Nov 1968.
3. Kanaan, A. E., and Powell, G. H., "DRAIN-2D . . . Inelastic Dynamic Response of Plane Structures," NISEE/Computer Applications, University of California, Berkeley, CA, 1973.
4. Ramberg, W., and Osgood, W. R., "Description of Stress-Strain Curves by Three Parameters," Technical Note 902, NACA, July 1943.
5. Jennings, P. C., "Periodic Response of a General Yielding Structure," Journal of the Engineering Mechanics Division, ASCE, Vol. 90, No. EM2, April 1964, pp. 131-166.
6. Wakabayashi, M., "Frames Under Strong Impulsive, Wind or Seismic Loading," Proceedings of the International Conference on Planning and Design of Tall Buildings, Lehigh University, Bethlehem, PA, 21-26 Aug 1972.
7. Plummer, F. B., "A New Look at Structural Energy Dissipation," Technical Report M-82, Construction Engineering Research Laboratory, Champaign, IL, 1974.
8. Martin, John F., "Cyclic Mechanical Tests and an Appropriate Analytical Stress-Strain Model for A36 Steel," Technical Report M-86, Construction Engineering Research Laboratory, Champaign, IL, 1974.
9. Landgraf, R. W., Morrow, J., and Endo, T., "Determination of the Cyclic Stress-Strain Curve," Journal of Materials, Vol. 4, No. 1, March 1969, pp. 176-188.
10. Morrow, J., "Cyclic Plastic Strain Energy and Fatigue of Metals," Internal Friction, Damping, and Cyclic Plasticity, ASTM STP 378, American Society for Testing and Materials, 1965, pp. 45-87.
11. Iwan, W. D., "On a Class of Models for the Yielding Behavior of Continuous and Composite Systems," Journal of Applied Mechanics, Vol. 34, No. 3, Sept 1967, pp. 612-617.
12. Popov, E. P., and Benter, V. V., "Cyclic Loading of Steel Beams and Connections," Journal of the Structural Division, ASCE, V. 99, No. ST6, June 1973, pp. 1189-1204.
13. McNamara, J. F., "Numerical Solution Techniques for Highly Non-linear Static Structural Behavior," Proceedings of the 1974 Army Numerical Analysis Conference, Philadelphia, PA, 12-14 Feb 1974.

14. McNamara, J. F., and Marcal, P. V., "Incremental Stiffness Method for Finite Element Analysis of the Nonlinear Dynamic Problem," Int. Symposium on Numerical and Computer Methods in Structural Mechanics, Urbana, IL, Sept 1971.
15. Marcal, P. V., "Finite Element Analysis of Combined Problems of Nonlinear Material and Geometric Behavior," Division of Engineering, Brown University, Report N00014-007/2, June 1969.
16. Nickel, R. E., "Direct Integration Methods in Structural Dynamics," Journal of Engineering Mechanics Division, ASCE, V. 99, No. EM2, April 1973, pp. 303-317.
17. Goudreau, G. L., and Taylor, R. L., "Evaluation of Numerical Integration Methods in Elastodynamics," Computer Methods in Applied Mechanics and Engineering, Vol. 2, 1972, pp. 69-97.
18. McNamara, J. F., "Solution Schemes for Problems of Nonlinear Dynamics," to be published, Journal of Pressure Vessel Technology, ASME.
19. Houbolt, J. C., "A Recurrence Matrix Solution for the Dynamic Response of Elastic Aircraft," Journal of Aeronautical Sciences, Vol. 17, 1950, pp. 540-550.
20. Bathe, J. E., and Wilson, E. L., "Stability and Accuracy Analysis of Direct Integration Methods," International Journal of Earthquake Engineering and Structural Dynamics, Vol. 1, 1973, pp. 283-291.
21. Newmark, N. M., "A Method of Computation for Structural Dynamics," Journal of the Engineering Mechanics Division, ASCE, Vol. 85, No. EM3, July 1959, pp. 67-94.
22. Martin, J. F., Topper, T. H., and Sinclair, G. M., "Computer Based Simulation of Cyclic Stress-Strain Behavior with Applications to Fatigue," Materials Research and Standards, ASTM, Vol. 11, No. 2, Feb 1971, pp. 23-29.
23. Jhansale, H. R. and Topper, T. H., "An Engineering Analysis of the Inelastic Stress Response of a Structural Metal Under Variable Cyclic Strains," Cyclic Stress-Strain Behavior - Analysis, Experimentation and Failure, ASTM STP 519, 1973, pp. 246-270.
24. Zienkiewicz, O. C., The Finite Element Method in Engineering Science, McGraw-Hill Publishing Co. Limited, London, 1971.
25. Felippa, C. A., "Refined Finite Element Analysis of Linear and Nonlinear Two-Dimensional Structures," Ph.D. Thesis, University of California, Berkeley, CA, 1966.
26. Toridis, T. G., and Khozeimeh, K., "Inelastic Response of Frames to Dynamic Loads," Journal of the Engineering Mechanics Division, ASCE, Vol. 97, No. EM3, June 1971, pp. 847-863.